AFRL-AFOSR-VA-TR-2017-0084

CRYOGENIC PELTIER COOLING

Joseph Heremans
OHIO STATE UNIVERSITY THE
190 N OVAL MALL
COUMBUS, OH 43210-1321

04/06/2017
Final Report

Air Force Research Laboratory
AF Office Of Scientific Research (AFOSR)/RTB1

REPORT DOCUMENTATION PAGE

Form Approved
OMB No. 0704-0188

1. REPORT DATE *(DD-MM-YYYY)*	2. REPORT TYPE	3. DATES COVERED *(From - To)*
06-04-2017	Final Performance	15 Sep 2010 to 14 Sep 2016

4. TITLE AND SUBTITLE
CRYOGENIC PELTIER COOLING

5a. CONTRACT NUMBER

5b. GRANT NUMBER
FA9550-10-1-0533

5c. PROGRAM ELEMENT NUMBER
61102F

6. AUTHOR(S)
Joseph Heremans

5d. PROJECT NUMBER

5e. TASK NUMBER

5f. WORK UNIT NUMBER

7. PERFORMING ORGANIZATION NAME(S) AND ADDRESS(ES)
OHIO STATE UNIVERSITY THE
190 N OVAL MALL
COUMBUS, OH 43210-1321 US

8. PERFORMING ORGANIZATION REPORT NUMBER

9. SPONSORING/MONITORING AGENCY NAME(S) AND ADDRESS(ES)
AF Office of Scientific Research
875 N. Randolph St. Room 3112
Arlington, VA 22203

10. SPONSOR/MONITOR'S ACRONYM(S)
AFRL/AFOSR RTB1

11. SPONSOR/MONITOR'S REPORT NUMBER(S)
AFRL-AFOSR-VA-TR-2017-0084

12. DISTRIBUTION/AVAILABILITY STATEMENT
DISTRIBUTION A: Distribution approved for public release.

13. SUPPLEMENTARY NOTES

14. ABSTRACT
This MURI aimed to improve efficiency and temperature range in thermoelectric (TE) Peltier cooling by improving the materials' 'figure of merit', or ZT. We established both the Ntype (BiSb:K) and the Ptype (YbPd2Pt) materials with the highest ZT's published in the temperature range. We established baseline ZT's for many other material classes usable in this range (the tetradymites and in particular Bi2Te2Se:Sn, which we then used to develop topological insulators). New heavyFermion materials emerged (CeAl2). FeSb3 performance was ascribed to phonon drag, and is unsuitable for cooling. New areas of research emerged in TE properties of Bibased nanowires.

15. SUBJECT TERMS
PELTIER, COOLING

16. SECURITY CLASSIFICATION OF:			17. LIMITATION OF ABSTRACT	18. NUMBER OF	19a. NAME OF RESPONSIBLE PERSON
a. REPORT	b. ABSTRACT	c. THIS PAGE			WEINSTOCK, HAROLD

Standard Form 298 (Rev. 8/98)
Prescribed by ANSI Std. Z39.18

DISTRIBUTION A: Distribution approved for public release.

Unclassified	Unclassified	Unclassified	UU	**PAGES**	**19b. TELEPHONE NUMBER** *(Include area code)* 703-696-8572

(1). Administration information

Grant Number: FA9550-10-1-0533
CRYOGENIC PELTIER COOLING
Ohio State University/Princeton University/Massachusetts Institute of Technology/Boston College/Michigan State University/California Institute of Technology/University of Houston
Project Director: Joseph P. Heremans, Ohio State University (Ohio Eminent Scholar, Mechanical Engineering, Physics)
Princeton PI: Robert Cava (Chemistry)
Massachusetts Institute of Technology PIs: Mildred S. Dresselhaus (Physics), Gang Chen (Mechanical Engineering)
Boston College PI: Cyril Opeil (Physics)
Michigan State University PI: Donald T. Morelli (Materials and Chemical Engineering)
California Institute of Technology: G. Jeffrey Snyder (Materials Science)
University of Houston PI: Zhifeng Ren (Physics)

(2). Program objective/scientific approach

This program is aimed at developing the fundamental science and technology to provide solid-state cooling in the 10 K to 150 K temperature range. The ultimate temperature difference that each stage of a Peltier cooler can achieve, and the thermodynamic efficiency of a Peltier cooler, are a function of essentially one material parameter, the *thermoelectric figure of merit* $zT=T\ S^2\sigma/\kappa$, where T is the average temperature of operation, S is the thermopower or Seebeck coefficient, and σ and κ are the electrical and thermal conductivity respectively. The goal of the program is to conduct research into new materials and new physical phenomena that will lead to an enhancement of zT.

The difficulty is that the materials parameters S, σ and κ are mutually counter-indicated, i.e. any change made to increase one almost always results in a decrease of another: increasing the electron concentration to increase σ decreases S by a fundamental relation, called the Pisarenko relation. Increasing the degree of disorder in the solid to decrease κ almost always decreases σ. The problem involves the study of transport properties of both the electrons, which dominate S and σ, and of the phonons, which dominate κ.

The scientific approaches used in this MURI are categorized into two classes:

(1) Increase S for a given σ by band structure engineering: indeed, it is known that a sharp local increase at a specific energy of the electronic density of states (DOS) leads to an optimal product $S^2\sigma$ [G.D. Mahan and J.O. Sofo, *Proc. Natl. Acad. Sci.* **93**, 7436 (1996)]. This is done specifically by using (1a) resonant dopants in semiconductors; (1b) semiconductors based on transition metals, where the *d*-levels of select atoms create the desired DOS; (1c) heavy Fermion metals, where the *f*-levels of rare earths create the desired DOS; and (1d) size quantization.

(2) Decrease κ for a given σ by nanostructuring, thus creating defects of one particular length scale so as to scatter phonons but not electrons. This is done (2a) by

developing heat-treatments during the casting of ingots of TE semiconductors; (2b) by mechanical nanostructuring using ball-milling and Spark Plasma Sintering.

The materials that were the focus of the initial efforts (but these have evolved over the duration of the program), were selected for having the best *zT* at the onset of the program:

(1) $Bi_{1-x}Sb_x$ alloys, very narrow-gap semiconductors. The *n*-type materials had the best $zT \leq 0.5$ at the onset of the program [B. Lenoir et al., *J. Phys. Chem. Solids* **59,** 129 (1998).] and the *p*-type materials reached $zT \leq 0.08$ at the onset of the program. [Y.S. Hor and R.J. Cava, *J. Alloys Compd.* **479,** 368 (2009).]

(2) Tetradymite semiconductors, of the general formula $(Bi_{1-x}Sb_x)_2(Te_{1-y}Se_y)_3$, which are used in commercial Peltier coolers, and in the six-stage Peltier coolers that reach the lowest cryogenic temperatures to date (about 180 K).

(3) Heavy Fermion metals [G.D. Mahan and J.O. Sofo, *Proc. Natl. Acad. Sci.* **93**, 7436 (1996).]

(4) Semiconductors with transition metal atoms as principal constituents, initially $FeSb_2$ [A. Bentien et al., *EPL* **80,** 17008 (2007).]

(3). The most recent program review (date, location, and government participants)

Title: "Cryogenic Peltier Cooling 4th Year Review Meeting"
Date: 3 May 2015 – 5 May 2015
Location: Kirtland Air Force Base, Albuquerque, NM
Government attendees: Dr. Harold Weinstock AFOSR/RSE; Dr. Charles Stein AFOSR/Kirtland AFB (ret.); Col. William Cooley, Chief of the Space Vehicles Directorate, AFRL; Douglas Dudis, WPAFB; Keith Avery, Kirtland AFB; William Byrne, Kirtland AFB.
MURI team members in attendance: Joseph P. Heremans (OSU); Robert Cava (Princeton); Mildred S. Dresselhaus and Gang Chen (MIT); Cyril Opeil (BC); Zhifeng Ren (UH); Donald T. Morelli (MSU); G. Jeffrey Snyder (Caltech); numerous post-doctoral fellows and graduate students supported by the program.

(4). Financial execution

The period of performance and funding is as follows:

Initial Award Increment #1 (2 months) 9/14/10-11/14/10 $271,257
Increment #2 (12 months) 11/15/10-11/14/11 $1,500,000
Increment #3 (12 months) 11/15/11-11/14/12 $1,500,000
Increment #4 (10 months) 11/15/12 - 9/14/13 $1, 228,743
Increment #5 (2 months) 9/14/13 – 11/14/13 $294,537
Increment #6 (12 months) 11/15/13 – 11/14/14 $1,500,000
Increment #7 (10 months) 11/15/14 – 9/14/15 $1,205,463

TOTAL FUNDING TO DATE: $7,500,000

In this MURI program as each increment of funds is added, the funds are split to be approximately OSU 25%, Princeton 12.5%, Michigan State 12.5%, Cal Tech 12.5%, Boston College/University of Houston 18.75% (split 28.5%/71.5%), and MIT 18.75%. Expenditure rates are consistent with the rate of incremental funding.

(5). Accomplishments to date:

5a Transport theory

5a.1 Electron transport

Heavy Fermion systems are believed to be good candidates for thermoelectric cooling applications at low temperature because of the sharp features of density of states near the Fermi level, which gives rise to good Seebeck coefficients. In combination with nanostructuring process, which drastically reduces the lattice thermal conductivity, such systems hold promise of possessing high ZT values. To understand the effects of nanostructuring on electron transport in heavy Fermion systems, thermoelectric properties in a Kondo insulator nanowire were investigated by the Chen group at MIT. The bulk electronic transport are simulated within the framework of Dynamic Mean Field Theory (DMFT), showing very small electron mean free paths, which indicates the electron properties can be preserved in nanostructures, while the phonons with longer mean free paths can be strongly scattered by the interfaces due to classical size effects. Both effects contribute to high ZT values up to 1.5 even at low temperatures. The results have been published by Nano Letters.

We are investigating the potential of using modulation doping and anti-resonance scattering in core-shell nanoparticles to improve the electron performance. Initial simulation shows that this is a promising direction.

Experimentally, a characterization system was built to study electron transport in thermoelectric material below room temperature. The setup is capable of measuring electrical conductivity, Seebeck, Hall, and isothermal Nernst coefficients from 4K to 350K. The measured transport coefficients can be analyzed to find energy dependence of electron scattering, density-of-states effective mass, Fermi level and electron's mobility. To validate the system, nano-grained $Bi_2Te_{2.7}Se_{0.3}$ sample was tested and the measured electrical conductivity and Seebeck coefficients match well with ones measured by a commercial characterization system (ULVAC ZEM3) at 300K with discrepancy less than 5%. This experimental setup will be applied to nano-grained BiSb alloys.

5a.2 Lattice thermal conductivity from first principles

We have applied first principles calculation to simulate phonon thermal conductivity and mean free path in materials of interests to our program, including Bi, Sb, and $FeSb_2$.

Bi-Sb alloy is one of the best thermoelectric materials for refrigeration applications. To control coupled transport of electrons and phonons and to enhance zT further, it is essential to understand their transport in the material. However, in bismuth and Bi-Sb alloy, phonon contribution to the total thermal conductivity is not well known since electrons and phonons have comparable contributions to total thermal conductivity.

To quantify phonon thermal conductivity and understand phonon transport in bismuth, we calculated lattice dynamics in bismuth using first principles and the Boltzmann equation which was very accurate in the case of other thermoelectric materials such as Si-Ge alloy. The calculated lattice thermal conductivity matches very well with the previous experimental work in low temperature range. Also, phonon mean free path, which is important for designing nanostructure sizes to enhance phonon scattering, was successfully calculated. From the calculation, we found three interesting features of phonon transport in bismuth. First, the 9^{th} nearest neighbors in the structure cannot be ignored even though the interatomic distance is long. This peculiar feature originates from the rocksalt-like crystal structure of bismuth and large electronic polarizability, and significantly affects both harmonic and anharmonic interactions between atoms. Second, the previous work about lattice thermal conductivity of bismuth estimated that lattice thermal conductivity is much smaller than electronic thermal conductivity near room temperature. However, according to our calculation, lattice thermal conductivity is comparable to the electronic thermal conductivity near room temperature. Therefore, the nanostructure approach to reduce thermal conductivity by enhanced phonon scattering may be still effective for bismuth. Last, bismuth is well-known for its anisotropic electron transport properties, but phonon transport in bismuth is almost isotropic. This may be due to small distortion of its crystal structure from exact rocksalt structure.

$FeSb_2$ has been intensively studied recently as a promising candidate for low temperature thermoelectric applications for its extremely large Seebeck coefficient around 10K, while the thermoelectric efficiency is limited by its high thermal conductivity. We have been studying the thermal transport properties of $FeSb_2$, including the thermal conductivity and especially the phonon mean free path, from first-principles simulations, aiming at providing a guideline to reduce the thermal conductivity of $FeSb_2$ by nanostructuring. We extracted the second and the third order force constants between atoms in the lattice from the force-displacement data calculated using density functional theory (DFT). The information of the second order force constants enabled the calculation of the phonon dispersion, which was in good agreement with that calculated using alternative density functional perturbation theory (DFPT). Anharmonic properties of $FeSb_2$ can be deduced from the third order force constants, based on which we obtained the temperature-dependent thermal expansion coefficient that matches well with the experimental data. To validate the third order force constants, we calculated the mode Grüneisen parameters from the extracted force constants and compared with those calculated using DFPT. Good agreement was observed and the calculated thermal conductivity was found in decent agreement with experimental data when the sample boundary scattering was also taken into account at low temperatures. The phonon mean free paths were also extracted, which indicated there is enough room for nanostructuring to reduce phonon thermal conductivity.

5b Experimental investigations of Heavy Fermion metals

The Morelli group at MSU has been interested in exploring thermoelectric effects below room temperature in alloys comprised of elements containing f-shell electrons. It is well known [G.D. Mahan and J.O. Sofo, *Proc. Natl. Acad. Sci.* **93**, 7436 (1996).] that a delta-function-type electron transport distribution function can maximize the thermoelectric properties by providing simultaneously large electrical conductivity σ and large Seebeck coefficient α. While such a distribution is not rigorously found in nature, it can be approximately achieved in alloys comprised of elements with f-shell valence electrons; these electrons form a narrow band in the density of states near the Fermi level. We have chosen to focus initially on two families of compounds: i) those based on $CePd_3$; and ii) those based on $YbAl_3$. The primary reasons for this choice are firstly, that these two base compounds possess the largest power factors ($\alpha^2\sigma$) of known compounds in the cryogenic temperature regime, and secondly they offer both p-type and n-type behavior, respectively, a necessary requirement for the development of a Peltier cooler.

A large part of our work up to this point has focused on identifying and implementing mechanisms for reducing the lattice thermal conductivity by compositional and structural modification, while at the same time maintaining large power factor. We have explored three separate approaches for increasing phonon scattering in these materials:

- *Solid solution formation*. This includes $Ce_{1-x}Sc_xPd_3$, $CePd_{3-x}Pt_x$, $Yb_{1-x}Sc_xAl_3$, and $Yb_{1-x}(RE)_xAl_3$, where RE = Lu or Er;
- *"Resonant" scattering by filler atoms*. This includes $CePd_3M_x$, with M = Al, Ga, Si, and Ge;
- *Nanostructure-induced phonon scattering in $CePd_3$.*

5b.1 $CePd_3$-based materials

1. The $CePd_3$ crystal structure (isostructural with $AuCu_3$) is shown in Figure 1. The total thermal conductivity is a sum of electronic and lattice (phonon) contributions; the latter can be modified by solid solution formation, as differences between the mass and size of substituted atoms can give rise to increased phonon scattering. Since $ScPd_3$ is isostructural with $CePd_3$, and Sc and Ce have a large mass difference, one might expect solid solutions of $Ce_{1-x}Sc_xPd_3$ would exhibit lattice thermal conductivity reduction. Instead, on samples with x ranging from zero to 0.25, we find [S.R. Boona and D.T. Morelli, *Journal of Electronic Materials* **41**, 1199 (2012).] that the lattice thermal conductivity is practically unchanged, a behavior suggesting that the Ce site plays a negligible role in phonon propagation. Substituting Pd for Pt, on the other hand, gives rise to the classic reduction in lattice thermal conductivity. At the same time, the Seebeck coefficient is hardly changed at all with substitution, behavior we attribute to the close ion size match between Pd and Pt, allowing for the preservation of the intermediate valent state that gives rise to large Seebeck coefficient. As a result (Figure 2), the figure of merit $ZT = (\alpha^2\sigma)T/\kappa$, is increased for the solid solution alloys and reaches values rivaling the best p-type materials below room temperature. [S.R. Boona and D.T. Morelli, *Appl. Phys. Lett.* **101**, 101909 (2012).]

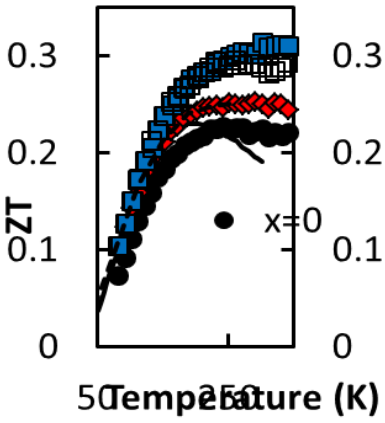

Figure 2. Thermoelectric figure of merit in the $CdPd_{3-x}Pt_x$ solid solution. The value of > 0. is the world record for a p-type material at 100 K.

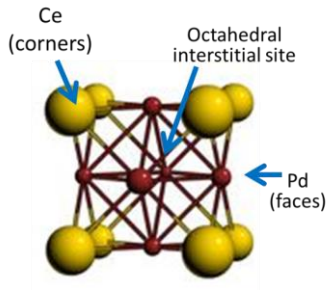

Figure 1. The $YbAl_3M_x$ structure. Large red circles: Yb; large open circles: Al; small filled circle: M ions.

A second and distinct approach [S.R. Boona and D.T. Morelli, *J. Appl. Phys.* **112**, 063709 (2012).] investigates structural modification by forming alloys of the form $CePd_3M_x$ ($0 \leq x \leq 1$). Here the M atom occupies a vacant body-centered void position in the $AuCu_3$ lattice (Figure 1). Such "filling" of large voids in structures is known to strongly affect the physical properties, and especially the thermoelectric properties, the skutterudites being a case in point. We find, again, a strong reduction in thermal conductivity that saturates with both filling fraction and filler mass. Unfortunately, the filled structures invariably exhibit depressed Seebeck coefficient, and the figure of merit is enhanced only slightly at 100K.

2. Finally, we have investigated whether nanostructuring of $CePd_3$ can lead to enhanced thermoelectric properties, primarily through thermal conductivity reduction via interface scattering of phonons. [S.R. Boona and D.T. Morelli (in preparation).] Again, this approach results in very effective reduction in thermal conductivity. However, the delicate intermediate valence state giving rise to high Seebeck coefficient is perturbed in

nanostructured materials, likely due to an increasing fraction of trivalent Ce at nanocrystal surfaces and grain boundaries.

3. An important outcome of the $CePd_3$-based work is the development of some basic strategies for reducing thermal conductivity while maintaining high Seebeck coefficient. [S.R. Boona and D.T. Morelli, *Journal of Electronic Materials* DOI 10.1007/s11664-012-2328-7 (2012).] For instance, Seebeck coefficients and power factors can be enhanced, though modestly, using chemical pressure, temperature, or doping; our continuing and future efforts are focused on combining these effects with some of the thermal conductivity reduction mechanisms described above in materials systems similar to $CePd_3$.

5b.2 $YbAl_3$-and $YbAl_2$-based materials

Efforts in the $YbAl_3$ compound family have primarily focused on the influence of substitutions on the Yb site. Solute ions included Sc, Lu, and Er. Representative results are described here for the $Yb_{1-x}Sc_xAl_3$ solid solution. We devised a novel method for synthesis of these compounds that involves a combination of arc-melting, annealing, etching, and powder processing that allows for the fabrication of this alloy family for the first time. [G.J. Lehr and D.T. Morelli, *Intermetallics* **32**, 225 (2013).] Substitution of Sc results in a drastic reduction in electrical resistivity and Seebeck coefficient; the resistivity of pure $ScAl_3$ is on the order of that of pure Al, and the Seebeck coefficient is near zero. Interestingly, however, for intermediate values of x, the Seebeck coefficient drops much less rapidly with Sc concentration, and as a result, at intermediate compositions, the power factor is enhanced over pure $YbAl_3$. At the same time, the increase in electronic thermal conductivity is counterbalanced by the expected reduction in lattice thermal conductivity due to alloy scattering. Taken together, this leads to an increase of the figure of merit by some 30% (Figure 3). Similar results are obtained using Lu and Er. [G.J. Lehr and D.T. Morelli, *Journal of Electronic Materials* DOI 10.1007/s11664-012-2401-2 (2012).] Finally, because use of this material in a Peltier module will require mechanical property data, we have undertaken a study [R.D. Schmidt, E. D. Case, G. J. Lehr, and D. T. Morelli, *Intermetallics* **35**, 15 (2013).] of the elastic modulus, shear modulus, and Poisson's ratio of these compounds and studied the effects

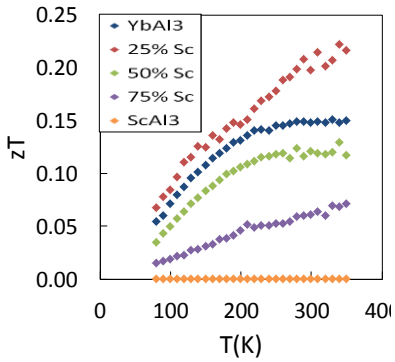

Figure 3. Thermoelectric figure of merit in the $Yb_{1-x}Sc_xAl_3$ solid solution

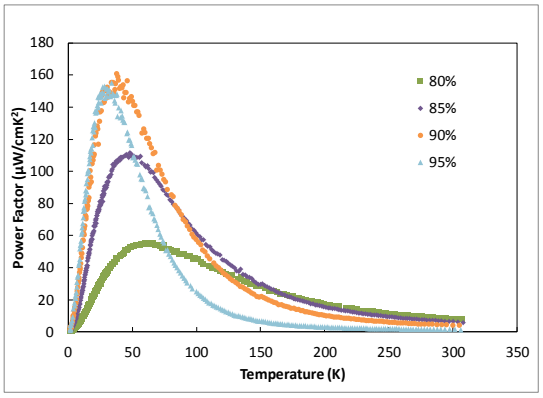

Figure 4. Thermoelectric power factor in the $Yb_{1-x}Sc_xAl_2$ solid solution

of porosity in powder processed samples on these mechanical parameters.

In parallel with the investigations on $YbAl_3$, we have also explored thermoelectric effects in the $Yb_{1-x}Sc_xAl_2$ family. [G.J. Lehr and D.T. Morelli (in preparation).] This alloy is of interest because, unlike the case of $YbAl_3$, substitution of Sc in $YbAl_2$ increases the lattice constant and drives the Yb ions to a more intermediate valent state and thus has the potential for increasing the Seebeck coefficient. Our preliminary investigations on this alloy family show that indeed this is the case. As can be seen in Figure 4, both the Seebeck coefficient (not shown) and the power factor increase dramatically as the Sc concentration is increased up to 90%, before falling slightly; additionally, the temperature of the peak value in the power factor shifts to lower temperature with increasing Sc. Both of these observations are consistent with a narrowing of the Kondo resonance peak in the f-electron density of states of this system. It is interesting to note that large power factor does not require large numbers of Yb ions – rather, only that they be spatially separated sufficiently to maximize the Kondo resonance. This result is interesting and potentially important as it gives us a means of tuning both the magnitude of the power factor and the temperature at which the maximum occurs, which can be made to coincide with the required temperature of operation of a Peltier cooler. While the ZT of this system does not exceed 0.1, it is hoped that this concept can be applied to other intermediate valence systems with larger potential figures of merit.

5c $Bi_{1-x}Sb_x$ alloys

Based on their bulk properties, bismuth antimony (BiSb) alloys with low Sb concentration are expected to be the materials showing the best currently known thermoelectric (TE) properties at temperatures below 77 K, the temperature of liquid nitrogen. The work on these alloys falls in three categories:

5c.1 Bulk and single crystal alloys doped with resonant impurities, which is further broken down into work on n-type and work on p-type alloys

5c.2 Quantum confined structures

5c.3 Bulk nanostructured composites

5c.1 Bulk and single crystal alloys doped with resonant impurities

5c.1.1 n-type single crystalline $Bi_{1-x}Sb_x$ alloys (OSU):

First principles calculations on various impurities in Bi were done by our collaborator, Bartlomiej Wiendlocha at AGH University of Science and Technology (Krakow, Poland). Among those impurities, Potassium (K) was found to be a promising resonant impurity in Bi while Lithium (Li) was predicted to be an n-type dopant if it goes into interstitial sites. Figure 1(a) shows that K introduces a sharp peak in density of states (DOS) of Bi near E_F which resembles the known resonant Tl peak in PbTe. [C.M. Jaworski, B. Wiendlocha, V. Jovovic and J.P. Heremans, *Energy and Environ. Sci.*, **4**(10), 4155 (2011).] From this result, it is expected that if K impurity level is hybridized into the extended state of host Bi, it will increase DOS of Bi where its sharp peak is located.

When E_F hits the distorted DOS, the resonant effect will appear in transport properties. Fig. 1(b) indicates that Li tends to increase E_F when it takes the interstitial sites in Bi.

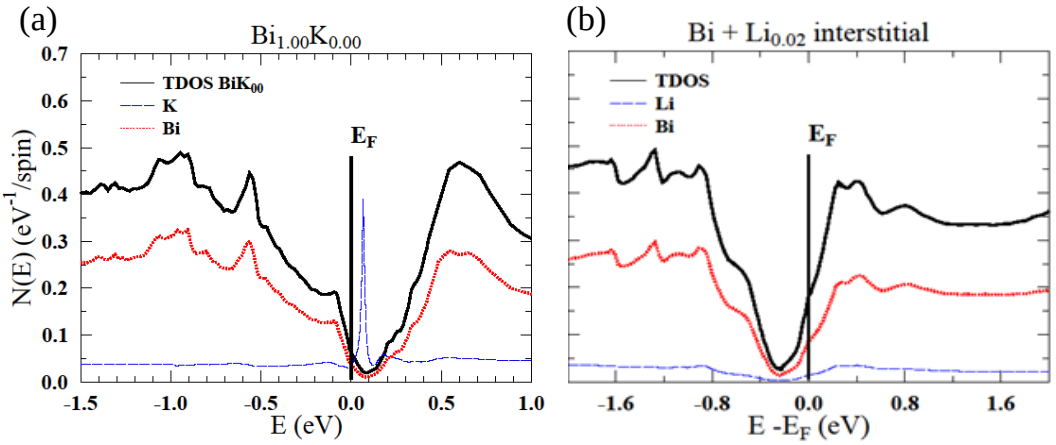

Figure 1. First principles calculations for Density of States of Bi with **(a)** K impurity and **(b)** Li impurity in interstitial sites

The band structure of $Bi_{1-x}Sb_x$ alloys is very similar to that of Bi except that $Bi_{1-x}Sb_x$ with $0.07<x<0.22$ has a band gap while Bi has the band overlap between the conduction band at the L-point and the valence band at the T-point. Therefore, the behavior of K and Li in $Bi_{1-x}Sb_x$ alloys is anticipated to be similar to that in Bi. The calculation of the DOS of $Bi_{1-x}Sb_x$ alloys with K and Li impurities is underway. Fig. 2 shows the experimental data on thermoelectric (TE) properties of K doped $Bi_{1-x}Sb_x$ samples compared to the undoped sample. It is obvious that K introduces an anomaly in *S*, exhibiting an additional hump at 20K and much larger *S* at lower temperatures. For $Bi_{93}Sb_7$ + 0.1% K sample, the power factor is increased by almost 2 times compared to the undoped sample and as a result, *zT* is enhanced about 50% from 100K up to 300K, reaching the maximum ~0.7 at 120K which is a record value up to date.

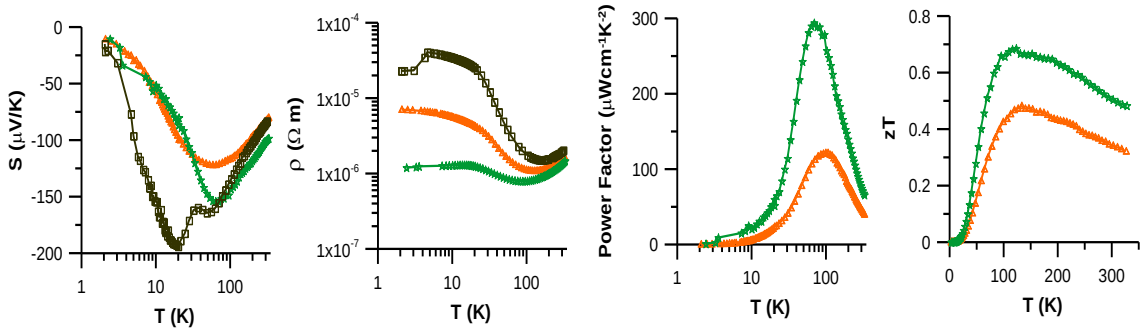

Figure 2. Seebeck coefficient (*S*), Electrical resistivity (ρ), Power factor, and *zT* of $Bi_{89.5}Sb_{10.5}$ (Orange), $Bi_{93}Sb_7$ + 0.1%K (Green), and $Bi_{90}Sb_{10}$ + 1%K (Dark green) samples. The values ZT>0.5 set the world record for n-type materials in this temperature range.

S and ρ of the undoped $Bi_{88}Sb_{12}$ and 1% Li doped $Bi_{88}Sb_{12}$ single crystal samples are presented in Fig. 3. [C.M. Orovets, A.M. Chamoire, H. Jin, B. Wiendlocha and J.P. Heremans, *Journal of Electronic Materials* **41**, 1648 (2012).] The Li doped sample shows metallic behavior compared to the undoped sample. These experimental results

confirm that Li actually goes into the interstitial sites in $Bi_{88}Sb_{12}$ so it acts as a strong n-type dopant.

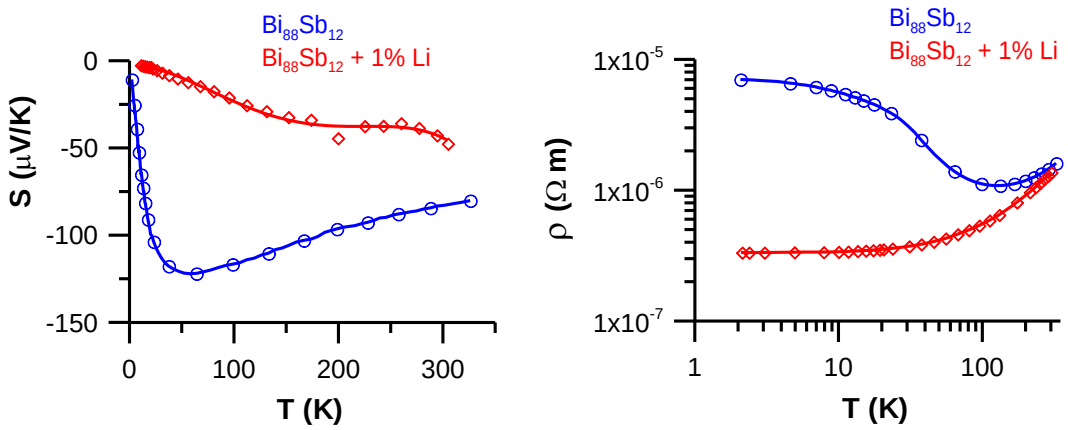

Figure 3. Seebeck coefficient (S) and Electrical resistivity (ρ) of $Bi_{88}Sb_{12}$ (Blue), and $Bi_{88}Sb_{12}$ + 1%Li (Red)

5c.1.2 p-type single crystalline $Bi_{1-x}Sb_x$ alloys:

There are two main results obtained so far for p-type single crystalline $Bi_{1-x}Sb_x$ alloys. Firstly, Indium (In) was found to be a new acceptor in Bi and $Bi_{1-x}Sb_x$ alloys which is surprising since In is the same trivalent element as Bi. Fig. 4 shows that Shubnikov de-Haas (SdH) measurements reveal that In increases the hole concentration in Bi.

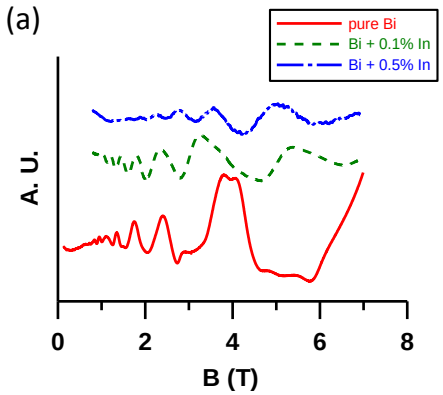

(b)

Samples	$[\Delta(1/H)]^{-1}$ (T)	A_F (m^{-2})	E_F (meV)	N_h (cm^{-3})
Bi	6.352	6.06×10^{16}	11.5	2.93×10^{17}
Bi + 0.1% In	7.665	7.31×10^{16}	13.9	3.88×10^{17}
Bi + 0.5% In	12.09	1.15×10^{17}	21.9	7.69×10^{17}

Figure 4. **(a)** Shubnikov de-Haas (SdH) oscillations in the electrical resistivity for pure Bi, Bi+0.1% In, and Bi+0.5%In samples. The oscillations are periodic in *1/H* where *H* is the magnetic field intensity. **(b)** Analysis results from SdH oscillations from (a) where A_F is the cross sectional area of the Fermi surface, E_F the Fermi level, and N_h the hole carrier concentration. It is obvious that In introduces additional holes in Bi.

Secondly, it was shown [H. Jin, C.M. Jaworski and J.P. Heremans, *Appl. Phys. Lett.* **101**, 053904 (2012).] that doping multiple valence bands can enhance the TE performance of p-type $Bi_{1-x}Sb_x$ alloys (Figure 5).

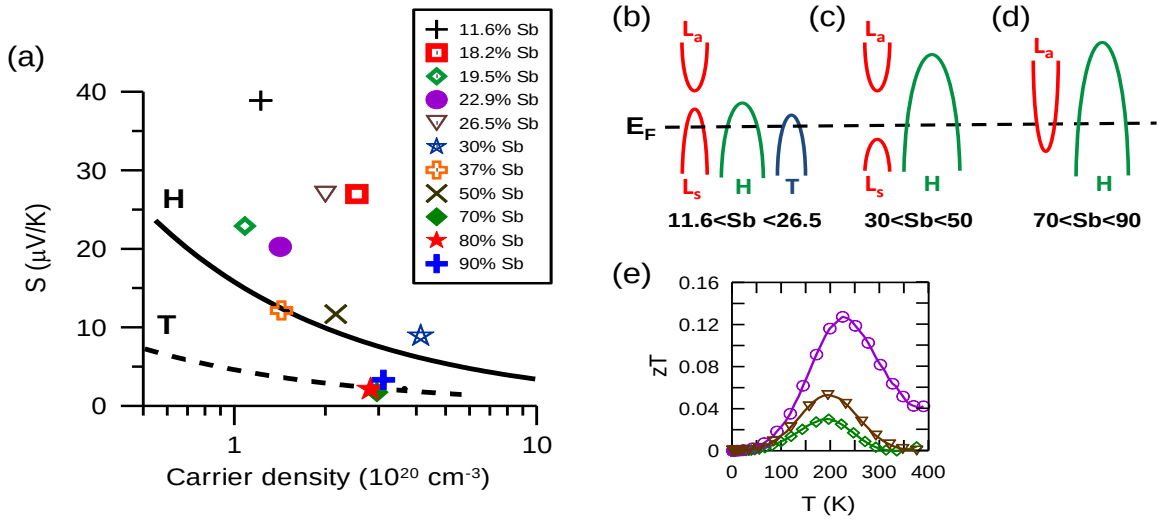

Figure 5. **(a)** Pisarenko's plot of thermopower versus hole concentration at *T*=80K for all measured samples in this study. Solid line and dashed line are calculated for the valence bands at the H-points and the valence band at the T-point, respectively. Points are experimental data. Carrier density of each sample was obtained from Hall measurement. **(b), (c), (d)** Schematic band diagrams for the three different Sb concentration regimes shown. **(e)** Samples with highest zT are presented. Those samples correspond to the case (b) and show thermopower above the calculated Pisarenko's line.

5c.2 Quantum confined $Bi_{1-x}Sb_x$ alloys structures at MIT

Since further enhancements of TE properties comes from quantum confinement effects, further TE enhancement is expected in thin film BiSb alloys, which as films also show the best three dimensional packing for nano-structured materials. However, the transport properties of BiSb alloys are very anisotropic. For these reasons, we have spent the past 2.5 years calculating various aspects of the electronic structure of BiSb thin films as a function of crystal orientation, thickness and temperature up to 77K. These calculations are now being extended to finding and optimizing the pertinent thermoelectric properties. With the start of the final two years of the program, we have added a postdoctoral researcher to grow appropriate samples and to make thermoelectric measurements as a function of Sb concentration in the BiSb alloys, their crystal orientation, film thickness and temperature. The following text gives details on the ongoing theoretical and experimental programs and their coupling.

5c.2.1 Theoretical Work on quantum confined $Bi_{1-x}Sb_x$

The Dresselhaus group has theoretically studied the electronic band structure properties of BiSb thin films as a function of film growth orientation, film thickness, and stoichiometry for the cryogenic temperature range. We have developed a general model for the low-dimensional narrow-band-gap material systems, where only the lowest conduction band and the highest valence band are important for the transport properties. The model for a BiSb thin film system is an iterative-two-dimensional-two-band model. Firstly, the two-band model describes the narrow-band-gap and the non-parabolic dispersion relation in bulk Bi and bulk BiSb alloys with remarkable accuracy. Because of the special properties of Bi and BiSb materials, the de Broglie wavelength of electrons in these materials is ultra-long, so that quantum size effects become obvious even when the film thickness is as large as 100 nm. Thus, it is difficult to carry out first principles calculations, such as density functional theory calculations, to model the Bi and BiSb thin films, due to the heavy computation caused by both the nano- and alloy-effects. To solve this problem, we developed an iterative approach to use the two-band model to study the two-dimensional (2D) system. The narrow-band-gap and

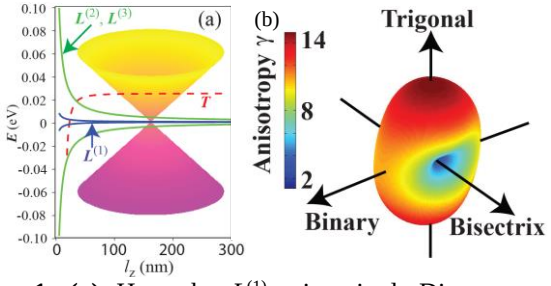

Fig. 1. (a) How the $L^{(1)}$-point single-Dirac-cone is formed. The figure shows the band structure of a $Bi_{0.96}Sb_{0.04}$ thin film grown normal to the bisectrix axis and how the band structure changes over different film thicknesses. The green curves show the lowest conduction band (upper one) and the highest valence band (lower one) at the $L^{(2)}$ and $L^{(3)}$ points in the Brillouin zone. The blue curves are for the $L^{(1)}$ point. The dashed red curve is the highest valence band at the T point. The $L^{(1)}$-point band gap remains less than ~1 meV until the film thickness l_z < 80 nm. The $L^{(2)}$ and $L^{(3)}$ points have the same band gap, which is largely opened up. Thus, an anisotropic single-Dirac-cone is formed at the $L^{(1)}$ point when the film thickness l_z is large enough to retain the $L^{(1)}$-point mini-gap at values less than ~1 meV. **(b)** How to control the electronic anisotropy of the Dirac-cone systems of $Bi_{1-x}Sb_x$ thin films. A general scheme of how the Fermi velocity ($\mathbf{v}_F$) anisotropy coefficient $\gamma = |\mathbf{v}_{max}|/|\mathbf{v}_{min}|$for the $L^{(1)}$-point single Dirac cone changes with film growth orientation. The value of γ for a specific film growth orientation is shown by the radius and the color on the left scale. γ can be as large as ~14, and as small as ~2. According to our calculations, γ is sensitive neither to the film thickness *l*, nor to the Sb composition *x* in the range of $0 < x < 0.15$.

the non-parabolic dispersion relations are obtained when the iterations come to convergence. This iterative-two-dimensional two-band model may be extended to a more general iterative low-dimensional-N-band model, if needed.

From our simulations, we theoretically point out the possibility of constructing different types of Dirac-cone materials based on BiSb thin films, as seen in Fig. 1. We found that we can engineer the band structure of BiSb as a function of the film stoichiometry, growth orientation, and thickness. We predict that it is possible to construct Dirac cones with different degrees of anisotropy and topology numbers, such as single-Dirac-cone materials, bi-Dirac-cone materials and tri-Dirac-cone materials as in Fig. 2a-c. Furthermore, we also predict how to construct quasi-Dirac-cone materials with different magnitude mini-band-gaps, and how to construct semi-Dirac-cones, where the electrons are linearly dispersed in one direction and parabolically dispersed in the other direction, as described in Fig. 2d.

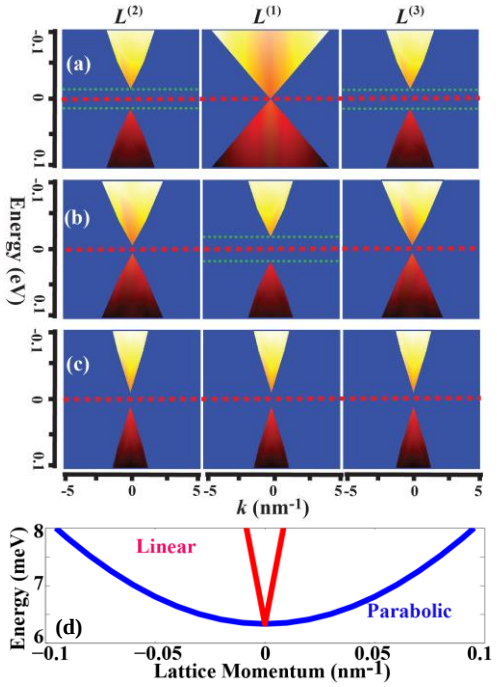

Fig. 2. An illustration of **(a)** single-**, (b)** bi- and **(c)** tri-Dirac-cone $Bi_{1-x}Sb_x$ thin films grown respectively along the **(a)** bisectrix, **(b)** binary and **(c)** trigonal axes. The illustration is based on the example of $Bi_{1-x}Sb_x$ thin films with film thickness $l = 100$ nm, $x = 0.04$, $P = 1$ atm and $T < 77$ K, under which the L points of bulk $Bi_{1-x}Sb_x$ have a zero-gap.**(d)** Example of a semi-Dirac cone in the $Bi_{1-x}Sb_x$ thin film system ($x = 0.10$ and $l = 100$ nm). We see that around the $L^{(1)}$ point, the fermions are linearly dispersed along the $\mathbf{v}_{max}$ direction, and parabolically dispersed along the $\mathbf{v}_{min}$ direction.

To guide thin film crystal growers, we have drawn out the electronic phase diagrams, in Fig. 3, as a function of film growth orientation, film thickness, and stoichiometry, based on our theoretical calculations, which include semi-metal (SM) phases, direct semi-conductor (DSC) phases and indirect semi-conductor phases (ISC). Finally, we have calculated the overall band gap and band overlap, as a function of film growth orientation, film thickness and stoichiometry in Fig. 3d-f. Furthermore, to control the properties of these cryogenic thermoelectric materials, we calculated the carrier concentration as a function of film orientation, film thickness, stoichiometry, and Fermi level in Fig. 4, to study their different transport properties. Future theoretical work will be focused on modifying our model to account for the measured results and for calculating thermoelectric properties in detail.

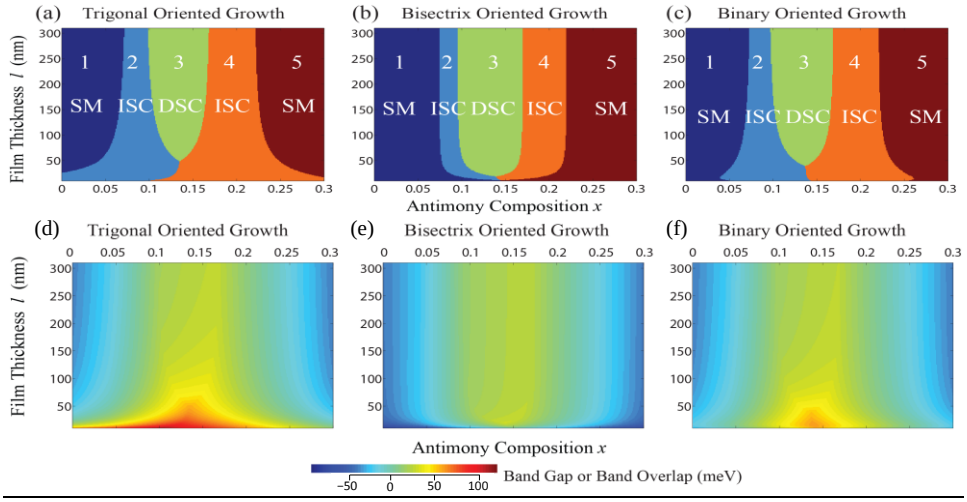

Fig. 3. (a-c) Phase diagrams of $Bi_{1-x}Sb_x$ thin films for different growth orientations as a function of film thickness and stoichiometry. The regions of semi-metal (SM), indirect-semiconductor (ISC), and direct-semiconductor (DSC) phases are shown explicitly. **(d-f)** The diagrams of overall narrow-band-gap and band overlap of $Bi_{1-x}Sb_x$ thin films for different growth orientations as a function of film thickness and stoichiometry. The magnitude of the band gap for a semiconductor phase is positive, while the magnitude of the band overlap for a semi-metal phase is negative.

5c.2.2 Experimental Work on quantum confined $Bi_{1-x}Sb_x$

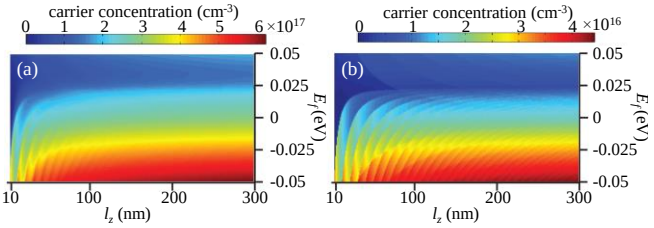

Fig. 4. Carrier concentration of $Bi_{0.96}Sb_{0.04}$ vs. film thickness l_z and Fermi level E_f are shown at **(a)** 77 K and **(b)** 4.2 K.

Experimental verification of various theoretically predicted Dirac cones in BiSb hinges on controlling the thin film crystal orientation. Since the films are Bi rich, we focus first on studying the growth dynamics of Bi. Previous techniques of fabricating Bi and BiSb thin films made samples with the trigonal axis perpendicular to the substrate, by lattice matching Bi to a supporting substrate (e.g. Mica or BaF_2). The key to growing high quality thin films is the choice of substrate and growth conditions (e.g. deposition technique, temperature, and pressure).

Thin Bi films were deposited on Mica using both thermal evaporation (TE) and molecular beam epitaxy (MBE). Figure 5a and 5b shows atomic force microscopy images of both types of films (~20 nm thick). The TE deposited film has grain boundaries that are shaped as triangles, which are characteristic of films grown along the trigonal direction. The MBE grown films, however, produce a much more diverse array of grain boundary shapes. This indicates that there is a mixture of crystallographic orientations.
We use MBE to study the impact of the substrate on the growth because MBE provides a more diverse set of grains. We grew Bi films on Si (111), Si (001), and sapphire substrates. The sapphire substrate stood out as having larger and more triangular grains than either Si substrate (Fig. 5c and 5d). To investigate the differences, we took x-ray diffraction (XRD) spectra (see Fig. 5e). From these spectra we identify two different preferred crystal orientations. One is the trigonal (001) (coordinates for Bi are given

using rhombohedral indices, as shown in Fig. 5) and the other is along the (012) direction. From the relative heights of the (001) and (012) peaks, we see that sapphire produces more trigonal oriented grains when compared with Bi films grown on Si. This result is expected since sapphire is better lattice matched to Bi than Si. Still, the results demonstrate that the choice of substrate based on the lattice mismatch can lead to growth of different crystal orientations.

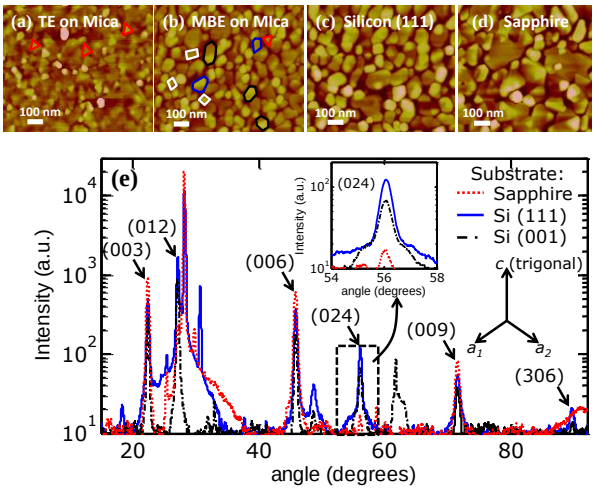

Fig. 5. Atomic force microscopy (AFM) images of ~20 nm thick Bi films. **(a)** Bi film deposited by thermal evaporation (TE) produces triangular grains (characteristic of the trigonal axis) on the order of ~100 nm. **(b)** Bi film grown by molecular beam epitaxy (MBE) produces grains of various shapes also on the order of ~100 nm. A few grains are outlined to guide the eye. AFM images of MBE grown Bi thin films on a **(c)** Si (111) and **(d)** sapphire substrate. The Bi grains on sapphire are larger and consist of more triangles. **(e)** X-ray diffraction spectrum of Bi film grown on sapphire, Si (111), and Si (001). The two primary crystal orientations of the Bi in a rhombohedral basis (a_1,a_2,c) are the trigonal face (001), and (012). The inset shows a close-up of the (024) peak, indicating that Bi grown on sapphire exhibits the smallest peak here, since its grains are primarily oriented along the trigonal axis.

5c.2.3 Future directions of the work on Bi films and quantum-confined structures

Since the substrate plays a critical role in defining the crystal orientation of the film, we will fine tune the substrate lattice parameters. BaF_2 has been shown to be an excellent match to trigonal oriented Bi films. To change the lattice constant of BaF_2 itself, we can grow a different material and use it as a buffer layer between BaF_2 and our supporting substrate. The gradually applied strain from the buffer layer will slightly change the lattice constant of the BaF_2.

Once samples are produced, we will use transport measurements and spectroscopic techniques to search for grains with quasi-Dirac cones. Gated structures will be fabricated, which will allow us to sweep the Fermi level through the electronic bands. All thermo-electric relevant properties will also be measured. Thermal conductivity can be measured using optical reflectance techniques. The Seebeck coefficient can be measured by using micro-fabricated platforms to simultaneously bias the device while monitoring temperature and heat flow. Finally, all results will be used to calibrate our theoretical models. This will allow us to theoretically optimize film thicknesses, operating temperatures, and doping concentrations. Theoretical modeling will be coordinated with experimental findings.

5c.3 Nanostructuring of $Bi_{1-x}Sb_x$ at Caltech

The reduction of thermal conductivity, specifically lattice thermal conductivity, has been a technique used to increase the figure of merit in thermoelectric materials for over twenty years. The reduction is achieved by scattering of phonons at the boundary between two different structures. However, this reduction is only beneficial if it is achieved while maintaining a power factor of approximately the same value or larger than if the structures did not exist. Here, the Caltech group focused on ways to incorporate a second phase into alloys of Bi-Sb in order to reduce the lattice thermal conductivity without significantly hindering the electron transport in the system.

Prior studies of Bi-Sb alloys exploited the use of grain size reduction to increase the overall figure of merit. The aim of this work was to use a metallurgical approach to improve the thermoelectric properties of $Bi_{90}Sb_{10}$. Concurrently, using bulk processing and consolidation techniques, this should act to improve the mechanical stability of these easily cleaved layered compounds as well.

Attempts using SnTe, Ag, and As have been made, with the most success involving precipitation of As samples. Typically, single crystal measurements are done both in the trigonal direction and perpendicular to in order to maximize zT, however we have focused on a subject not often studied, that is, the properties of polycrystalline Bi-Sb. The previous studies of polycrystalline Bi-Sb focusing on grain size reduction have never shown great promise because of the fact that the electron mobility is severely limited. However, the goal here is to maintain a large grain size, with a small enough structure size to adequately scatter phonons without debilitating the electron mobility.

In the past, two types of consolidation have been used. The first involves cold pressing and then sintering the material with the second involving hot extrusion of the cold pressed material. The density of often far below that of the theoretical density for samples that are cold pressed and sintered, and often times not reported in the literature. However, samples that were extruded after cold pressing had densities which approached that of the theoretical value. These samples were shown to have preferential orientation relative to the extrusion direction, resulting in texturing and directionally dependent properties. We have been working on utilizing our rapid induction heated hot press to achieve similar results to that of the extruded samples, but with the benefit of having little to not texturing.

Experimental Results

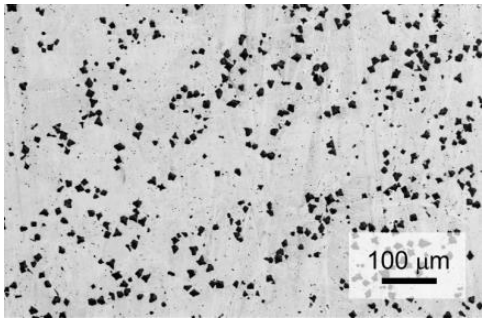

Figure 1. Scanning electron microscope (SEM) image in backscatter mode of Bi-SnTe sample melted and annealed

Initial attempts to nanostructure elemental bismuth with SnTe were unsuccessful due to the low temperatures necessary for the precipitation step. Typically, materials are melted, homogenized and then precipitated in three separate isothermal steps. However, since Bi has such a low melting temperature and the reaction kinetics are slow enough at the temperatures in which it was believed to be homogeneous that this attempt was unsuccessful.

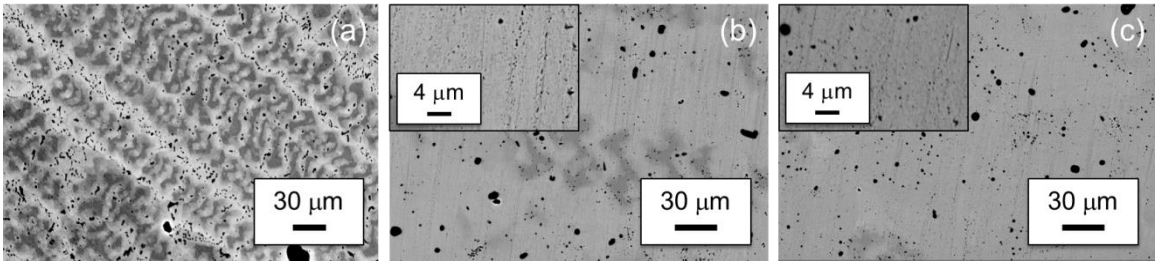

Figure 2. Electron microscope images of $Bi_{90}Sb_{10}$ with Ag: **(a)** melt, **(b)** 2 at. %, and **(c)** 4 at. % microstructure

As can be seen in Figures 3 and 4, both attempts at nanostructuring $Bi_{90}Sb_{10}$ were successful in creating second phase with the potential to effectively scatter phonons. Figure 5a shows the melt microstructure for the Ag added Bi-Sb sample. After annealing for 3 days at 250°C both the 2 at. % (Fig. 6b) and 4 at. % (Fig. 7c) Ag samples had similar microstructure. However, because of the doping effect of Ag in Bi-Sb alloys further measurements were not conducted.

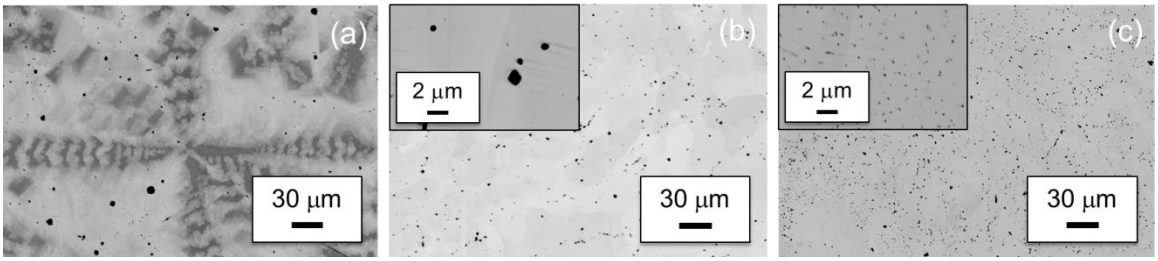

Figure 8. Electron microscope images of $Bi_{90}Sb_{10}$ with As: **(a)** melt, **(b)** 2 at. %, and **(c)** 4 at. % microstructure

The As structured samples, however, had a marked difference between the 2 at. % (Fig. 9b) and 4 at. % (Fig. 10c) microstructure. The large precipitates seen in Figure 11a are formed during melting step, however there is still a significant amount of As dissolved in the matrix that then phase segregates upon annealing at 250°C for three days.

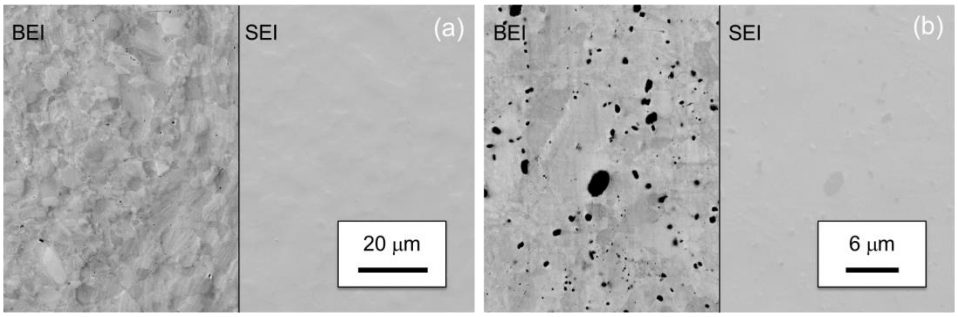

Figure 12. Electron microscope images of **(a)** consolidated $Bi_{90}Sb_{10}$ and **(b)** with 4 at. % As

There is an issue with precipitate coarsening during the rapid consolidation step as seen in Fig. 13. The consolidation parameters work well with regard to densification as the sample hot pressed without arsenic showed little to no porosity, with a density at or above 98% of the theoretical (Fig. 14a). However, the 4 at. % sample that was hot pressed showed a large amount of material coarsening (Fig. 15b). The fine microstructure seen in the inset of Fig 16c had coarsened and all of the fine microstructure was no longer present.

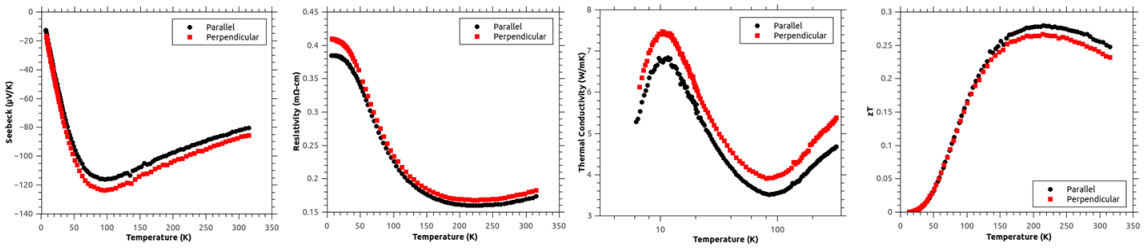

Figure 17. Transport measurements for pure $Bi_{90}Sb_{10}$ perpendicular and parallel to the pressing direction to establish the extent of texturing.

The resulting low temperature transport measurements revealed that the sample anisotropy seems to be minimal (Fig. 18). The property most problematic with regard to anisotropy is the thermal conductivity (Fig. 19c) as there is a drastic difference in the room temperature thermal conductivity. Based on the low temperature measurements conducted, this anisotropy is significantly reduced indicating little to no preferential orientation during hot pressing with both samples having comparable *zT* (Fig. 20d).

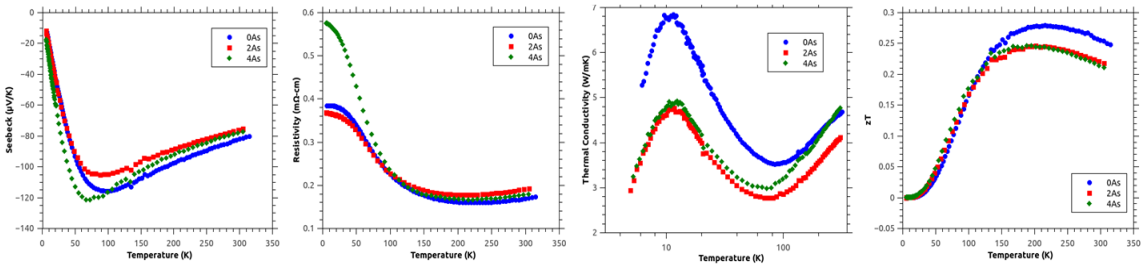

Figure 21. Low temperature transport measurements for pure $Bi_{90}Sb_{10}$, 2 at. % and 4 at. % arsenic structured samples.

The first round of low temperature transport measurements revealed that the arsenic structures do indeed reduce the thermal conductivity as expected (Fig. 22c). However, the results of the Seebeck and resistivity measurements (Fig. 23a-b) are difficult to explain solely from the transport measurements as each sample had an equivalent or near equivalent carrier concentration. It is believed that arsenic could be increasing the value of the band gap, but more work is required to determine if this is the case.

Conclusion

Successful microstructure formation has been attained in alloys of Bi-Sb. The current method for microstructure generation has proven successful at thermal conductivity reduction for samples structured in the range of 2-4 at. % arsenic. However, it is believe that these results can be improved by eliminating the precipitate coarsening

upon consolidation. This can potentially be remedied by annealing the samples for less time prior to consolidation. This is something that will be examined in the near future.

Once it has been established that the coarsening can be reduced during consolidation, continued coordination with the Ohio State group for the purpose of conducting low temperature transport measurements will be necessary to assess the extent to which the zT can be improved for the optimized samples.

Also to be examined is the possibility of band gap widening due to the addition of arsenic. This will be examined with respect to the lattice parameter change as characterized by x-ray diffraction.

5d Mechanical nanostruturing, particularly of $FeSb_2$

The MURI project activities at Boston College are a collaborative effort between the Opeil Group, which specializes in thermodynamic material characterization at cryogenic temperatures and the Ren Group responsible for sample materials preparation. The main thrust of our research combines the technique of nanostructured material preparation and the intriguing report of a large Seebeck coefficient (-45,000 μV/K) in single crystal $FeSb_2$. [Sun et al., *Dalton Trans*. **39**, 1012 (2010).] Our research efforts have focused on improving the thermoelectric performance (*ZT*) of $FeSb_2$ using the techniques of chemical doping, the integration of Cu and Ag nanoparticles [H. Zhao, et al., *Nanotechnology* **23**, 505402 (2012).], nanostructuring [H. Zhao et al., *Appl. Phys. Lett*. **99**, 163101 (2011).], and stoichiometric adjustment. [M. Pokharel et al. *MRS Proceedings* **1456**, 1505 (2012).] This research has led to significant improvements in thermoelectric efficiency, *ZT*, primarily through a significant reduction of thermal conductivity resulting from increased phonon scattering and a decrease in resistivity resulting from the introduction of Ag nanoparticles during the nanocomposite synthesis.

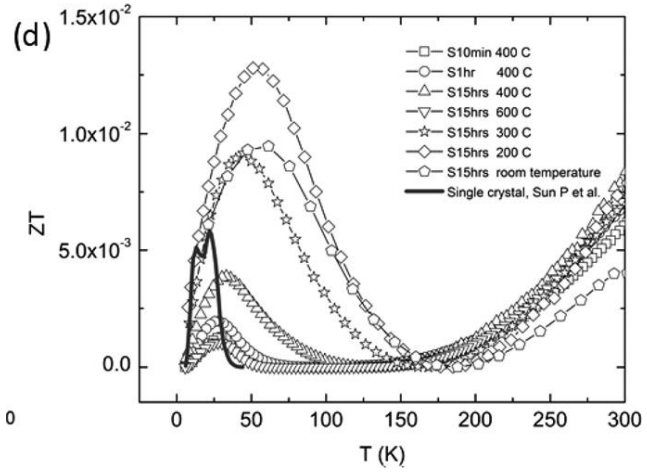

Figure 1. Comparison of the temperature dependent thermoelectric efficiency, *ZT*, of nanocomposite $FeSb_2$ with different grain sizes and $FeSb_2$ single crystal data from Sun, et al. J. Phys. Conf. Ser. 150, 012049 (2009). The optimized nanocomposite sample represents an increase of 160% over the single crystal performance, for further details see H. Zhao et al., *Appl. Phys. Lett*. **99**, 163101 (2011).

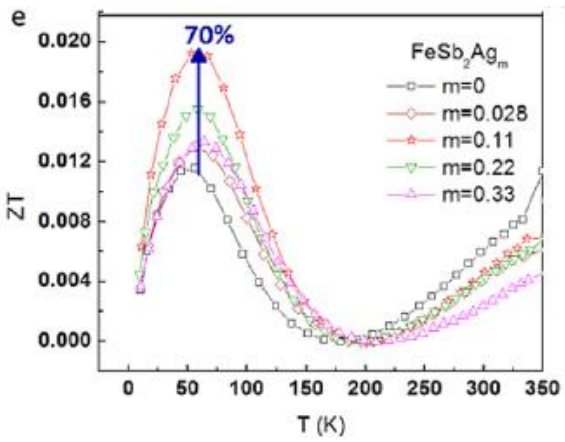

Figure 2. Temperature dependent thermoelectric efficiency, *ZT*, comparison for an increasing amount of Ag nanoparticles in the $FeSb_2$ nanocomposite matrix. The optimized *ZT* occurs for $FeSb_2Ag_m$ at m = 0.11 due to the metal/semiconductor interface engineering approach stemming from the similar work functions of $FeSb_2$ and Ag. This approach reduced both the thermal conductivity and resistivity. For details see, H. Zhao et al., *Nanotechnology* **23**, 505402 (2012).

In the following, the activities and accomplishments for the first two and a half years are summarized.

Note on Professor Zhifeng Ren's move to the University of Houston

As part of the MURI program on Cryogenic Cooling using thermoelectric materials led by Prof. Joseph Heremans at Ohio State University, Ren's group has carried out work on materials synthesis and characterizations at Boston College (BC) before the end of 2012. Starting from January 1 2013, his group moved from BC to University of Houston (UH). In the past two and a half years, his group has first doubled the *ZT* of the single crystals reported in literature in the first year by creating nanostructured $FeSb_2$ using ball milling and hot pressing technique his group developed over the last a few years, then doubled the doubled *ZT* in the second year by adding nanoparticles into the nanostructured $FeSb_2$. At UH, his group will continue to carry out the proposed work with enhanced intensity due to better facilities his group is setting up at UH.

5d.1 Preparation and characterization of nanostructured $FeSb_2$

Nanostructured $FeSb_2$ samples are made through ingot synthesis by melting, ball milling, and hot pressing processes. By optimizing the processing parameters, nanostructured $FeSb_2$ materials showed the lowest thermal conductivity of less than 1 W/mK that is much lower than the peak thermal conductivity of 500 W/mK of the single crystals, however the Seebeck coefficient also decreased drastically to about 125 μV/K, only a tiny fraction of the single crystals' 42,000 μV/K. Nevertheless, a thermoelectric figure-of-merit (*ZT*) of 0.013 was achieved, which is more than double of the state-of-the-art value of the single crystals. Interestingly the *ZT* curve is also dramatically broadened, which is very beneficial to the applications at a broader temperature range. In addition, doping in this material has also been studied.

5d.2 Preparation of nanostructured Bi-Sb alloy materials

The alloy was made by melting method. The nanostructured materials were prepared by ball milling and hot pressing. In addition, melt spinning was also used to synthesize Bi-Sb ribbons with the size of micrometers. In the process, we have added potassium (K) into the materials. Interesting results were found in the K-doped Bi-Sb polycrystalline materials. An enhancement of about 20% at 300 K on power factor from both the Seebeck coefficient and electrical conductivity was observed.

5d.3 Fabrication of nanostructured $FeSb_{2-x}Ag_x$ with nanoinclusions $Ag_{1-y}Sb_y$

Based on the result of enhanced thermoelectric figure-of-merit (*ZT*) of 0.013 on nanostructured $FeSb_2$ we achieved in 2011, we tried to further improve the *ZT* of nanostructured $FeSb_2$ through doping. Out of the many elements we have tried so far, we found that silver (Ag) provided some enhancement to the nanostructured $FeSb_2$. By replacing some Sb with Ag, we synthesized nanostructured $FeSb_{2-x}Ag_x$ with 10 % (molar ratio) nanoinclusions $Ag_{1-y}Sb_y$ with significant *ZT* enhancement comparing to the nanostructured pure $FeSb_2$. The experimental data show that both thermal conductivity and electrical resistivity of the nanocomposites were significantly reduced in the lower temperature regime comparing with pure $FeSb_2$ owing to the interfaces between $FeSb_{2-x}Ag_x$ and $Ag_{1-y}Sb_y$ phases, as well as the similar work functions between the two phases. Overall, significant improvement in *ZT* (from 0.013 to 0.019) was achieved for the optimized nanocomposite composition $FeSb_{1.975}Ag_{0.025}/Ag_{0.77}Sb_{0.23}$ in which $Ag_{0.77}Sb_{0.23}$ is about 10% by molar ratio. The results by this approach clearly demonstrated that metal/semiconductor interface played an important role and confirmed the potential of strongly correlated material systems as promising thermoelectric materials.

5d.4 *ZT* enhancement of nanostructured $FeSb_2$ by adding Cu nanoparticles

After the work done on Ag addition into $FeSb_2$, we realized that Cu may be even better than Ag since Cu does not react with $FeSb_2$ whereas Ag does. The isolated Cu nanoparticles can act as modulation dopant to provide the needed electrons in increasing the electrical conductivity without degrading the Seebeck coefficient. Sure enough, addition of Cu nanoparticles have made us to achieve nanocomposite $FeSb_2Cu_{0.045}$ with *ZTs* of 0.026, such a *ZT* value doubled our last year's record of 0.013, fulfilling the promise of *ZT* doubling every year since we started this MURI program in 2010.

5d.5 Investigation of other thermoelectric materials working at cryogenic temperatures

Aside from $FeSb_2$, we are also trying to find new materials, such as $CrSb_2$, which has been reported to having Seebeck coefficient of 5000 μV/K below 10 K. At the same time, we are also trying to synthesize another p-type material $CeCu_6$.

5d.6 Analysis of Phonon Drag in $FeSb_2$ Nanocomposite

In an attempt to understand the physics of the large Seebeck coefficient in $FeSb_2$, reported by Sun et al. [Sun et al., *Dalton Trans*, **39**, 1012 (2010).] we studied the thermal conductivity (κ) and Seebeck coefficient (S) of nanocomposites of varying grain size. The grain-size dependence of these properties and the correlations between the properties themselves reveals that phonon-drag contributes significantly to the large S-value of

coarse-grained samples. The severe degradation of S-peak for nanocomposites is a consequence of the suppression of the phonon-drag effect due to increased boundary scattering.

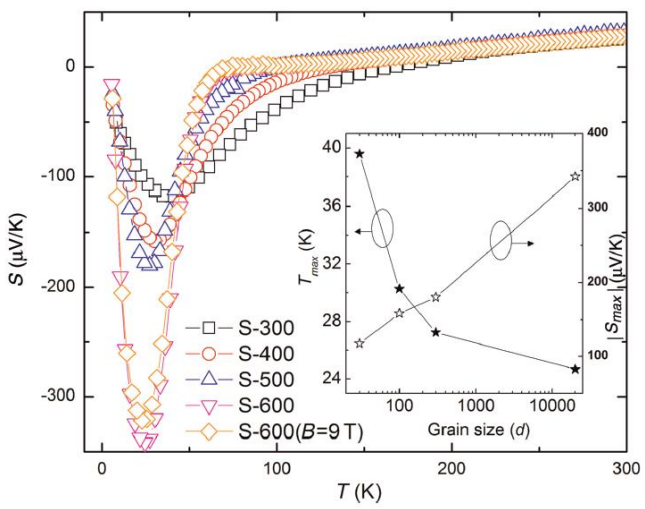

Figure 3. Temperature dependence of the Seebeck coefficient for the four different grain size samples. Fitting to the power law was done for all the samples below 50 K. Inset: Grain size dependence of the peak value (S_{max}) and the peak position (T_{max}) of the Seebeck coefficient. S_{max} for all samples is significantly small than that of a single crystal at low-T, whereas at high T the values are comparable. As shown in the inset, the S_{max} decreases with decreasing grain size. This is expected for the phonon-drag effect, because the non-electronic scattering reduces the phonon mean free path, which reduces the phonon-drag contribution.

Our nanocomposite data and analysis of phonon drag do not support other mechanisms that might explain the large Seebeck effects reported by Bentien et al. [A. Bentien et al., *Euro. Phys. Lett*. **80**, 17008 (2007).] Although one cannot preclude the presence of electron–electron correlation effects, their role in this phenomenon may be a minor one. The recent analysis of electron correlations using a hybrid functional approach of Becke [A.D. Becke, *J. Chem. Phys*. **98**, 1372 (1993).] and Hegin's GW functional approach [L. Hedin, *Phys. Rev*. **139**, A796 (1965).] by Tomczak et al. [J.M. Tomczak, *Phys. Rev*. B **82**, 085104 (2010).] suggest that the high thermopower in $FeSb_2$ should not be understood in the context of local correlations, but rather by utilizing vertex corrections to the transport coefficients. Such vertex corrections describe the phonon-drag effect. The phonon-drag effects in $FeSb_2$ are similar to those described in p-type Ge by Geballe and Hull. [T.H. Geballe and G.W. Hull, *Phys. Rev*. **94**, 1134 (1954).] In a similar vein the study of magnetoresistance and Hall effect by Takahashi et al. [H. Takahashi et al., *Phys. Rev*. B **84**, 205215 (2011).] concludes that the large Seebeck coefficient in $FeSb_2$ is unlikely to originate from electron–electron correlations because they have an insignificant effect on the Seebeck coefficient in the low-temperature insulating regime. Our data on $FeSb_2$ nanocomposite supports their conjecture that the phonon-drag effect plays an essential role in enhancing the Seebeck coefficient in the low temperature regime, as shown in other semiconductor materials e.g., InSb [H.P.R. Frederikse and E.V. Mielczarek, *Phys. Rev*. **99**, 1889 (1955).] and weakly P doped Si. [L. Weber and E. Gmelin, *Appl. Phys*. A **53**, 136 (1991).]

5d.7 Kapitza Resistance and Thermal Conductivity in $FeSb_2$ Nanocomposite

In further analyzing the strong grain-size dependent thermal conductivity of the $FeSb_2$ nanocomposites, we used a simple macroscopic model (effective medium

approximation, EMA) [D.A.G. Bruggeman, *Ann. Phys*. (Leipzig) **24**, 636 (1935); R. Landaure, *J. Appl. Phys*. **23**, 779 (1952).] based on Kapitza resistance calculation using equation, $(T,d) = \frac{\kappa_i}{1+\frac{2R_k\kappa_i}{d}}$, where κ_i is the intrinsic (or bulk) thermal conductivity, R_k is the Kapitza resistance and d is the grain size. Here κ_i is grain-size independent but is temperature dependent while $L_k = R_k\kappa_i$ and $G_k = \frac{1}{R_k}$ are called the Kapitza length and Kapitza conductance, respectively. In an effective medium approach, the total thermal conductivity of a polycrystal is the sum of the intra-grain and the inter-grain contributions. The inter-grain component arises due to the interfacial resistance, also known as the Kapitza resistance, to the thermal transport. In the presence of thermal gradient, the Kapitza resistance results in a temperature discontinuity across the interface, which was first roported by Kapitza [P.L. Kapitza, *J. Phys*. (Moscow) **4**, 181 (1941)]. The overall effect of the Kapitza resistance is to reduce the thermal conductivity and the effect is more pronounced at smaller grain sizes. Our analysis showed that the Kapitza length found for nanocomposite $FeSb_2$ at 10 K was 390 nm with a Kapitza resistance of the order of 10^{-7} m^2KW^{-1}, which confirmed the importance of interfacial thermal resistance across the grain boundaries in determining the thermal properties of nanocomposite $FeSb_2$ sample. Our thermal conductivity data shows the Kapitza resistance was the predominating factor in determining the bulk thermal properties below 50 K.

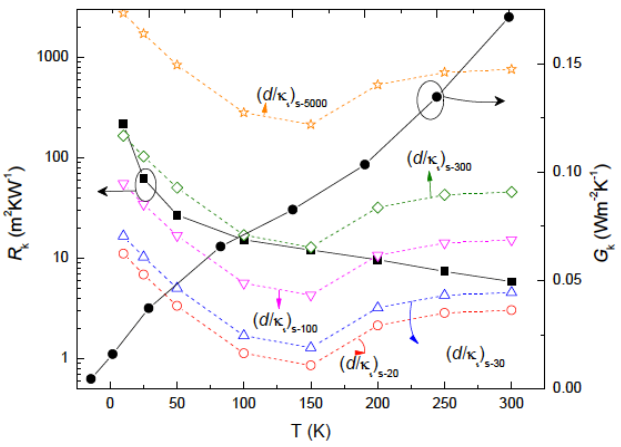

Figure 4. Temperature dependence of the Kapitza resistance (R_k) and Kapitza conductance (G_k) obtained as best fit to equation given above. R_k and G_k values are represented by left and right Y-axes, respectively. The open symbols with dashed lines represent the temperature dependence of the bulk thermal resistance (d/κ_i) as indicated by the left Y-axis for the five samples. Stars: S-5000, Diamonds: S-300, down-pointed triangles: sample S-100, up-pointed triangles: sample S-30, open-circles: sample S-20, filled circles: G_k (T), filled sq.: R_k (T).

5e The Thomson cooler derived from the Compatibility Factor Approach to the analysis of Thermoelectric Devices (Caltech)

Traditional thermoelectric Peltier coolers exhibit a cooling limit which is primarily determined by the figure of merit, zT. Rather than a fundamental thermodynamic limit, this bound can be traced to the difficulty of maintaining thermoelectric compatibility. Self-compatibility locally maximizes the cooler's coefficient of performance for a given zT and can be achieved by adjusting the relative ratio of the thermoelectric transport properties that make up zT. We investigated the theoretical performance of thermoelectric coolers that maintain self-compatibility across

the device. We find that such a device behaves very differently from a Peltier cooler, and we term self-compatible coolers "Thomson coolers" when the Fourier heat divergence is dominated by the Thomson, as opposed to the Joule, term. A Thomson cooler requires an exponentially rising Seebeck coefficient with increasing temperature, while traditional Peltier coolers, such as those used commercially, have comparatively minimal change in Seebeck coefficient with temperature. When reasonable material property bounds are placed on the thermoelectric leg, the Thomson cooler is predicted to achieve approximately twice the maximum temperature drop of a traditional Peltier cooler with equivalent figure of merit (zT).We anticipate that the development of Thomson coolers will ultimately lead to solid-state cooling to cryogenic temperatures. In order to make such a cooler new kinds of high Seebeck and low Seebeck materials are required. This opens up new challenges and opportunities for thermoelectric material development.

5f Tetradymites

At the outset, the bulk of our research of the Cava group at Princeton focused on improving the thermoelectric properties of state-of-the-art bismuth telluride selenide materials, which we attempted through several different approaches. However, by the present point in time we have shifted our focus towards a few other classes of materials as well, as discussed below. With regard to bismuth telluride selenide, we primarily concentrated on alloys that are selenium-rich (i.e., Bi_2Te_2Se and Bi_2TeSe_2) compared to the tellurium-rich state-of-the-art materials that have already been optimized through countless other studies [see e.g., D.M. Rowe, CRC Handbook of Thermoelectrics, CRC Press, 1995]. Because relatively Se-rich materials have received less attention in the literature, their defect chemistry is less understood and consequently less control over their properties has been achieved. Thus, our studies on these materials have sought to understand and control the defect chemistry and correspondingly the carrier concentrations in these materials, which directly affect the thermoelectric properties.

The work presented in [Shuang Jia et al., *Phys Rev B* **84**, 235206 (2011)] reports the characterization of the material Bi_2Te_2Se, which was synthesized by two different techniques – i.e., the modified Bridgman and Bridgman-Stockbarger (B-S) methods – and with different amounts of Te-excess/Se-deficiency. These crystals yielded different sets of electronic properties based on different concentrations of defects; in particular, it was noteworthy that crystals of low carrier concentrations (down to ~5×10^{14} cm^{-3} at 4 K) were achieved and could be grown consistently. Incidentally, this finding was of interest to the topological insulator community (which is also intently studying Bi-Te-Se compounds at present). Yet, the ability to achieve such a large extent of compensation in this material is also noteworthy from the perspective of our thermoelectrics research, and so we have pursued further investigations on this material. Specifically, we have spent the past year probing the homogeneity of B-S grown as well as Sn-substituted Bi_2Te_2Se crystals, and have collected a significant amount of thermoelectric data that have been drafted into a manuscript [M.K. Fuccillo, Shuang Jia, M.E. Charles, and R.J. Cava, Thermoelectric properties of Bi_2Te_2Se compensated by native defects and Sn doping] recently submitted to the Journal of Electronic Materials. An additional study [Shuang Jia et al., *Phys Rev B* **86**, 165119 (2012)] that we performed on Bi_2Te_2Se involved collaboration with the Princeton University Department of Physics to use scanning

tunneling microscopy to "see" and identify the defects in crystals of slight Bi-excess/Te-deficiency.

Another direction we set out on while studying the bismuth tellurides involved the material $Bi_2Te_{1.6}S_{1.4}$, which exhibits rich defect chemistry and electronic properties similar to those of Bi_2Te_2Se because of the stronger electronegativity of S atoms (like Se) compared to Te. Although we supported characterization of the material properties of this compound form a thermoelectrics perspective, $Bi_2Te_{1.6}S_{1.4}$ turned out to be more of interest as a topological insulator [Huiwen Ji & al., *Phys Rev B* **85** 201103(R) (2012)] than a thermoelectric material.

Yet another avenue we have pursued on Bi-Te-Se compounds was to consider the material Bi_2TeSe_2. The study outlined in [M.K. Fuccillo & al., *Solid State Communications* **152** 1208 (2012)] shows how we used Sb substitution for Bi to hole-dope and compensate a strongly n-type material to the point of an n-p crossover and then beyond it into the heavily-doped p-type side. We studied the effects of this substitution on the thermoelectric properties and found that the thermoelectric figure of merit over the composition range studied was highest near the crossover.

As is evident from the above, much of our work on the bismuth tellurides has supported topological insulator research. The influence of this work on that field has recently been discussed in a review article submitted to the Journal of Materials Chemistry [R.J. Cava & al. (Submitted to the Journal of Materials Chemistry)].

The Cava group has recently begun to shift focus towards studying $FeSb_2$-like and $MnTe_2$-like compounds as described in the MURI proposal and **section 5d** above. They have determined several different possible crystal growth methods to obtain pure and doped crystals of many of these materials, and a number of crystals have been successfully obtained. Electronic transport measurements and Investigations into the defect or other mechanisms (e.g., correlated electrons) giving rise to the transport and carrier concentrations in these compounds are presently ongoing, and some preliminary data was presented at the recent MURI meeting and discussed with collaborators. The next steps include trying to develop ways of controlling these properties.

6a Publications

In Press / In preparation

Z. Tian, S. Lee and G. Chen, "Heat Transfer in Thermoelectric Materials and Devices", *Journal of Heat Transfer* (accepted).

M. Koirala, H. Zhao, M. Pokharel, S. Chen, C. Opeil, G. Chen, and Z. Ren, "Thermoelectric Property Enhancement by Cu Nanoparticles in Nanostructured $FeSb_2$", (in preparation).

M.K. Fuccillo, Shuang Jia, M.E. Charles, and R.J. Cava, "Thermoelectric properties of Bi_2Te_2Se compensated by native defects and Sn doping." (Submitted to the Journal of Electronic Materials)

R.J. Cava, Huiwen Ji, M.K. Fuccillo, Q.D. Gibson, and Y.S. Hor, "Crystal Structure and Chemistry of Topological Insulators." (Submitted to the Journal of Materials Chemistry) http://arxiv.org/abs/1302.1059

2013

R.D. Schmidt, E.D. Case, G.J. Lehr, and D.T. Morelli, "Room temperature mechanical properties of polycrystalline $YbAl_3$, a promising low temperature thermoelectric material," *Intermetallics* **35**, 15 (2013).

G.J. Lehr and D.T. Morelli, "Synthesis, crystal structure, and thermoelectric properties of the $YbAl_3$-$ScAl_3$ solid solution," *Intermetallics* **32**, 225 (2013).

2012

J.P. Heremans, B. Wiendlocha and A.M. Chamoire, "Resonant levels in bulk thermoelectric semiconductors", *Energy Environ. Sci.* **5**, 5510 (2012).

C.M. Orovets, A.M. Chamoire, H. Jin, B. Wiendlocha and J.P. Heremans, "Lithium as an Interstitial Donor in Bismuth and Bismuth-Antimony Alloys", *Journal of Electronic Materials* **41**, 1648 (2012).

H. Jin, C.M. Jaworski and J.P. Heremans, "Enhancement in the figure of merit of p-type $Bi_{100-x}Sb_x$ alloys through multiple valence-band doping", *Appl. Phys. Lett.* **101**, 053904 (2012).

S.R. Boona and D.T. Morelli, "Thermoelectric properties of $Ce_{1-x}Sc_xPd_3$," *Journal of Electronic Materials* **41**, 1199 (2012).

S.R. Boona and D.T. Morelli, "Enhanced thermoelectric properties of $CePd_{3-x}Pt_x$," *Appl. Phys. Lett.* **101**, 101909 (2012).

S.R. Boona and D.T. Morelli, "Relationship between structure, magnetism, and thermoelectricity in $CePd_3M_x$ Alloys," *Journal of Applied Physics* **112**, 063709 (2012).

S.R. Boona and D.T. Morelli, "Structural, magnetic, and thermoelectric properties of some $CePd_3$-based compounds," *Journal of Electronic Materials* DOI 10.1007/s11664-012-2328-7 (2012).

G.J. Lehr and D.T. Morelli, "Thermoelectric properties of $Yb_{1-x}(Er,Lu)_xAl_3$ solid solutions", *Journal of Electronic Materials* DOI 10.1007/s11664-012-2401-2 (2012)

S. Tang and M.S. Dresselhaus, "Constructing Anisotropic Single-Dirac-Cones in $Bi_{1-x}Sb_x$ Thin Films", *Nano Letters* **9,** 2021 (2012).

S. Tang and M.S. Dresselhaus, "Phase Diagrams of $Bi_{1-x}Sb_x$ Thin Films with Different Growth Orientations", *Physical Review B* **86**, 075436 (2012).

S. Tang and M.S. Dresselhaus, "Constructing a Large Variety of Dirac-Cone Materials in the $Bi_{1-x}Sb_x$ Thin Film System", *Nanoscale* **4**, 7786 (2012).

N.A. Heinz, T. Ikeda, and G.J. Snyder, "Formation of highly oriented large nanoscale In2Te3 precipitates in bulk Bi2Te3", *Acta Materialia* **60**, 4461 (2012).

N.A. Heinz, S. Howell, H. Wang, T. Ikeda, and G.J. Snyder, "Hot pressing and nanostructuring of Bi90Sb10 alloys to concurrently improve mechanical and thermoelectric properties", *Physica Status Solidi (a)* **209**, 2565 (2012).

H. Zhao, M. Pokharel, S. Chen, B. Liao, K. Lukas, C. Opeil, G. Chen, and Z.F. Ren, "Figure-of-Merit Enhancement in Nanostructured $FeSb_{2-x}Ag_x$ with Nanoinclusions $Ag_{1-y}Sb_y$", *Nanotechnology* **23**, 505402 (2012).

Shuang Jia, Haim Beidenkopf, Ilya Drozdov, M.K. Fuccillo, Jungpil Seo, Jun Xiong, N.P. Ong, Ali Yazdani, and R.J. Cava, "Defects and high bulk resistivities in the Bi-rich tetradymite topological insulator $Bi_{2+x}Te_{2-x}Se$," *Phys Rev B* **86**, 165119 (2012) (editor's choice) http://prb.aps.org/pdf/PRB/v86/i16/e165119

Huiwen Ji, J.M. Allred, M.K. Fuccillo, M.E. Charles, M. Neupane, L.A. Wray, M.Z. Hasan, and R.J. Cava, "Bi2Te1.6S1.4: A topological insulator in the tetradymite family, *Phys Rev B* **85** 201103(R)" (2012) (rapid communication) http://prb.aps.org/pdf/PRB/v85/i20/e201103

M.K. Fuccillo, M.E.Charles, Y.S.Hor, Shuang Jia, and R.J. Cava, Low temperature thermoelectric properties of $Bi_{2-x}Sb_xTeSe_2$ crystals near the n-p crossover, *Solid State Communications* **152** 1208 (2012)
http://www.sciencedirect.com/science/article/pii/S0038109812002682#

2011

C.M. Jaworski, B. Wiendlocha, V. Jovovic and J.P. Heremans, "Combining Alloy Scattering of Phonons and Resonant Electronic Levels to Reach a High Thermoelectric Figure of Merit in PbTeSe and PbTeS alloys", *Energy and Environ. Sci.* **4**(10), 4155 (2011).

E. Rogacheva, D. Orlova, M.S. Dresselhaus and S. Tang, "Size Effects in Bi-Sb Solid Solutions Thin Films", *Materials Research Society Proceedings* **1314** (2011).

Y. Zhang, M.S. Dresselhaus, Y. Shi, Z.F. Ren, and G. Chen, "High Thermoelectric Figure-of-Merit in Kondo Insulator Nanowires at Low Temperatures", *Nano Letters* **11**, 1166 (2011).

H. Zhao, M. Pokheral, G. Zhu, S. Chen, K. Lukas, Q. Jie, C. Opeil, G. Chen, and Z.F. Ren, "Dramatic thermal conductivity reduction by nanostructures for large increase in thermoelectric figure-of-merit of $FeSb_2$," *Appl. Phys. Lett.* **99**, 163101 (2011).

Shuang Jia, Huiwen Ji, E. Climent-Pascual, M.K. Fuccillo, M.E. Charles, Jun Xiong, N.P. Ong, and R.J. Cava, "Low-carrier-concentration crystals of the topological insulator Bi2Te2Se", *Phys Rev B* **84**, 235206 (2011) (editor's choice)
http://prb.aps.org/pdf/PRB/v84/i23/e235206

6b Presentations

2013

G. Chen, "Thermoelectric Transport in Bulk and Nanostructured Materials," invited talk at Gordon Research Conference on Nanomaterials for Applications in Energy Technology, Ventura, California, February 3-8, 2013.

2012

J. P. Heremans, "Thermoelectric and spin-thermal solid state energy conversion", Nobel Symposium on Nanoscale Energy Converters (NS 153), Örenäs Castle, Skåne, Sweden, August 12-16, 2012.
http://www.nobelprize.org/nobel_organizations/nobelfoundation/symposia/physics/ns153/index.html

H. Jin, B. Wiendlocha, J.P. Heremans, "Thermoelectric properties of alkali-doped BiSb alloys and discovery of potassium as a resonant level", International Conference on Thermoelectrics, Aalborg, Denmark, July 2012.

H. Jin, B. Wiendlocha, J.P. Heremans, "Potassium is a good resonant level in BiSb alloys", Materials Research Society Spring Meeting, San Francisco, April 2012.

J.P. Heremans, H. Jin, B. Wiendlocha, "Potassium is a resonant level in $Bi_{1-x}Sb_x$ alloys", American Physical Society March meeting, Boston, Mar. 2012.

C.M. Orovets, H. Jin, B. Wiendlocha, J.P. Heremans, "Cryogenic Thermoelectric Properties of the Bismuth-Magnesium and Bismuth-Antimony-Magnesium Systems", American Physical Society March meeting, Boston, Mar. 2012.

S.R. Boona and D.T. Morelli, "Relationship between structure, magnetism, and thermoelectricity in $CePd_3M_x$ Alloys," Oral presentation, American Physical Society March Meeting, Boston, MA, 2012.

S.R. Boona and D.T. Morelli, "Structural, magnetic, and thermoelectric properties of some $CePd_3$-based compounds," Oral presentation, 31st International Conference on Thermoelectrics, Aalborg, Denmark, 2012.

S.R. Boona and D.T. Morelli, "Nanostructuring effects in $CePd_3$-based compounds," Oral presentation, Fall Meeting of the Materials Research Society, Boston, MA, 2012.

G.J. Lehr and D.T. Morelli, "Thermoelectric Properties of $Yb_{1-x}(Sc,Er,Lu)_xAl_3$ Solid Solutions," Poster presentation, 31st International Conference on Thermoelectrics, Aalborg, Denmark, 2012.

G.J. Lehr and D.T. Morelli, "A study of the relationship between intermediate valence and Seebeck coefficient in Yb-Al compounds," Oral presentation, Fall Meeting of the Materials Research Society, Boston, MA, 2012.

B. Liao, K. Esfarjani and G. Chen, "First-principles study of thermal transport in FeSb2", ASME International Mechanical Engineering Congress and Exposition, Houston, TX, Nov. 9-15, 2012.

B. Liao, M. Zebarjadi, K. Esfarjani and G. Chen, "Cloaking core-shell nanoparticles from conducting electrons in solids", poster presentation, Material Research Society Fall Meeting, Boston, MA, Nov. 25-30, 2012. Winner of the Student Poster Award for Thermoelectric Symposium.

S. Lee, K. Esfarjani, J. Garg, and G. Chen, "Lattice thermal conductivity of bismuth from first principles", Material Research Society Fall Meeting, Boston, MA, November 25-29, 2012.

G. Chen, "Thermoelectric Materials, Transport, and Applications," Keynote at Physics@FOM, Veldhoden, Netherland, January 17-18, 2012.

G. Chen, "Thermal Transport and Properties in Nanostructured Materials," Plenary lecture at 18th Symposium on Thermophysical Properties, Boulder, Colorado, June 24-29, 2012.

G. Chen, "Nanostructured Materials for Thermoelectric Energy Conversion," invited talk, ACS National Meeting, Philadelphia, August 18-23, 2012.

G. Chen, "Nanostructured Materials for Thermoelectric Energy Conversion," invited talk, Orcas 2012, International Conference on Energy Conversion and Storage, Friday Harbor, WA, September 4-6, 2012.

Z.F. Ren, "Solar Energy Conversion into Electricity and Hot Water by Thermoelectric Effect", ACP 2012, Guangzhou, China, Nov 7-10, 2012.

Z.F. Ren, "Aligned Carbon Nanotubes and Nanostructured Thermoelectric Materials", East Lake International Forum on Frontiers of Science and Technology for Outstanding Overseas Young Scholars, Wuhan, China, Oct. 6-8, 2012.

Z.F. Ren, "Nanomaterials, Physics, and Applications in Energy Research", Workshop on Energy and Advanced Information Materials, Shengzhong Lake, Sichuan, China, July 22-29, 2012.

Z.F. Ren, "Nanostructured Bulk High Temperature Thermoelectric Materials", MRS meeting, San Francisco, CA, USA, April 9-13, 2012.

Z.F. Ren, "Electron and Phonon Engineering in Nanostructured Thermoelectric Materials", The USC Smart Energy Summit, Los Angeles, CA, USA, Jan 27, 2012.

2011

H. Jin, B. Wiendlocha, J.P. Heremans, "Indium is an Acceptor in Bismuth", American Physical Society March meeting, Dallas, Mar. 2011.

S.R. Boona and D.T. Morelli, "Thermoelectric properties of $Ce_{1-x}Sc_xPd_3$," Poster presentation, 30th International Conference on Thermoelectrics, Traverse City, MI, 2011

Y. Tang, Poster presentation, 30th International Conference on Thermoelectrics, Traverse City, MI, 2011.

N. Heinz, Poster presentation, 30th International Conference on Thermoelectrics, Traverse City, MI, 2011.

Z.F. Ren, "Nanostructured Thermoelectric Materials", HI TEMP 2011 Conference, Boston, Massachusetts, USA, Sept 20-22, 2011.

Z.F. Ren, "2nd Status meeting SPP 1386 for Nanostructured Thermoelectrics", Wittenburg, Germany, July 4-6, 2011.

Z.F. Ren, "Nanostructured Thermoelectric Materials and Their Applications in Energy", MRS meeting, San Francisco, USA, April 25-28, 2011.

Z.F. Ren, "Nanostructure Approach for High-performance Thermoelectrics, Photovoltaics, and Biosensing", 2011 NES/APS-AAPT Joint Spring Meeting, UMass Lowell, Massachusetts, USA, April 8-9, 2011.

Z.F. Ren, "Nanostructured Thermoelectric Materials and Their Applications in Energy Conversion", Symposium on Nanophotonics and Renewable Energy, Beijing, China, Jan 16-18, 2011.

2010

H. Jin, C.M. Jaworski, J.P. Heremans, "p-type $Bi_{1-x}Sb_x$ above 300K", American Physical Society March meeting, Portland, Mar. 2010.

Colloquium and seminar presentations

Z.F. Ren, Boston University, Boston, Massachusetts, USA, "Why are nano materials useful for enhancing energy conversion?", November 18, 2011.

Z.F. Ren, University of Houston, Texas, USA, "Why are nanomaterials important to energy physics and engineering?", November 17, 2011.

Z.F. Ren, University of Maryland, Maryland, USA, "Why are nano materials useful for enhancing energy conversion?", October 26, 2011.

Z.F. Ren, University of North Carolina at Chapel Hill, North Carolina, USA, "Why nanostructure is important for future's energy need?", September 12, 2011.
Z.F. Ren, University of Science and Technology of China, Chengdu, China, "Nanostructure Approach for Enhancing the Thermoelectric Performance of Bulk Materials", July 7, 2011.

Z.F. Ren, Minzu University of China, Beijing, China, "Why nanostructure is important for the future's energy need?", June 1, 2011.

(7) Plans for the option years

So far, the MURI has set the record values of *zT* in the cryogenic temperature range, in both n-type materials (K-doped BiSb alloys) and p-type ($CePd_2Pt$) materials. These values will be consolidated (i.e. assessed for durability and repeatability), and enhanced.

Indeed the scientific directions taken have proven themselves fruitful, and yet new ideas have arisen. In the last two years, the following research plans will be enhanced or reduced.

- The work on tetradymites at Princeton will wind down; it will be replaced by additional work on the possible semiconducting heavy Fermion systems ($FeSb_2$-like) such as $RuSb_2$.
- The work on natural nanostructuring of $Bi_{1-x}Sb_x$ alloys at Caltech will decrease; it will be replaced by new work developing a new concept for cryogenic cooling based on the Thomson effect.
- The work on bulk $Bi_{1-x}Sb_x$ alloys at OSU and MIT will be enhanced, with the following focus points:
  (a) The experimental investigation of quantum structures (MIT) has just started and will become a focal point.
  (b) The exact compositions x and K-donor concentrations needed to develop resonances will need to be determined.
  (c) The effect of a moderate external magnetic field will be investigated.
  (d) Other possible resonant impurities will be explored.
  (e) A new idea based on the addition of microscopic (but not nanoscale) inclusions of insulting materials will be explored, in the hope of attempting to prepare material with (1) Dirac states following the MIT calculation (Dresselhaus-group) (2) the idea of "cloaked" core/shell inclusions following the MIT calculations (Chen-group).

(8) Transition planning

Given the progress to date of the values for ZT achieved by MURI team members, contacts are being initiated with AFRL scientists at the Space Vehicles Directorate, Kirtland AFB. Ms. Gloria Lehr, who is pursuing her Ph.D. research at Michigan State University, under the direction of Prof. Donald T. Morelli under this MURI program, and is the author of the work on n-type heavy Fermion systems based on Al_3Yb, applied to the Air Force Research Laboratory's Space Scholar Program.
Another change being planned is the move of Prof. Zhifeng Ren from Boston College to the University of Houston.

(9) Issues of concern

None

(10) Recommendation for funding

It is strongly recommended that this program be fully funded for the final 2 years.